BEAM DYNAMICS STUDIES FOR SRF PHOTOINJECTORS*

T. Kamps†, A. Neumann, J. Voelker
Helmholtz-Zentrum Berlin, Germany

Abstract

The SRF photoinjector combines the advantages of photo-assisted production of high brightness, short electron pulses and high gradient, low-loss continuous wave (CW) operation of a superconducting radiofrequency (SRF) cavity. The paper discusses beam dynamics considerations for ERL class applications of SRF photoinjectors. One case of particular interest is the design of the SRF photoinjector for BERLinPro, an ERL test facility demanding a high brightness beam with an emittance better than 1 mm mrad at 77 pC and average current of 100 mA.

MOTIVATION

The primary goal of this study is to design an electron injector within the boundary conditions of B*ERL*inPro [1]. For B*ERL*inPro, the electron injector needs to deliver an electron beam with a normalized emittance of $\varepsilon_{\rm n} = 1$ mm mrad and average current of $I_{avg} = 100$ mA. The rms pulse length must be $\sigma_t \leq 7$ ps in order to reduce emittance growth in the merger, linac and recirculation loop of the ERL. In addition the injector design should be compatible with technical boundary conditions. These translate into rf forward power limits set up by the rf power source and rf input coupler technology of choice. In particular the gun forward power is limited to $P_{\rm fd} = 230$ kW by the rf input coupler.s The secondary goal is to develop guidelines and requirements for the microwave desgin of the SRF cavity.

PRELIMINARIES

The main building blocks for the electron injector of B*ERL*inPro are an SRF gun with drive laser, solenoid and booster section (see Fig. 1). The solenoid and SRF cavity are located in a gun cryomodule. The beam exits the cryomodule and is guided through a short warm section with laser input and diagnostics ports before it enters the booster cryomodule. In this study beam parameters are first evaluated after the gun section at the location of the first booster cavity and finally after the booster section, before the beam enters the merger section. All beam dynamics simulations for this study have been carried out with the ASTRA code [2].

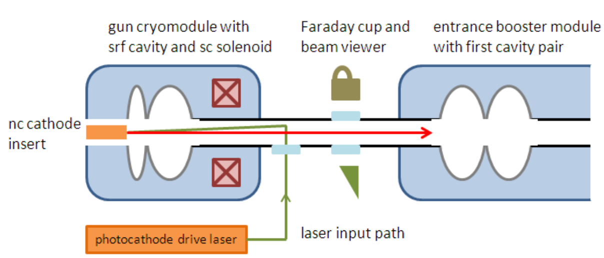

Figure 1: Schematic overview injector system with SRF gun and booster.

EMITTANCE CONTRIBUTIONS

The initial emittance for a beam from a photocathode RF gun is given by the product of initial spot size and the mean transverse energy distribution ($\mathrm{MTE} = (h\nu - \phi_{\rm eff})/3$) of the electron distribution after photoemission from the cathode with effective workfunction $\phi_{\rm eff}$ and single-photon energy $h\nu$ of the drive laser [3]. Low emittance requires a cathode material with a workfunction near the single-photon energy of the drive laser and small initial spot size. The lower limit for the initial spot size is given by the equilibrium between the forces of the image-charge and the accelerating field. This space-charge limited (scl) emission radius is a function of the ratio of bunch charge q_b and launch field E_l the bunch experiences during emission. The resulting thermal (or cathode) emittance and the lower limit for the emission spot size can be expressed by

$$\varepsilon_{\rm th} = \sigma_{\rm in}\sqrt{\frac{\mathrm{MTE}}{m_o c^2}} \quad \text{with} \quad \sigma_{\rm in}|_{\rm scl} = \sqrt{\frac{q_b}{4\pi\epsilon o E_l}} \qquad (1)$$

It is clear from Eq. (1) that a high launch field is required to achieve low thermal emittance for a given target bunch charge. The upper limit for the launch field is given by the cathode-to-peak field ratio (given by cavity design) and the achievable peak field in SRF gun cavity structures of $E_{pk} = 45$ MV/m [4]. For B*ERL*inPro we assume a drive laser running at $\lambda = 532$ nm illuminated a photocathode made of CsK_2Sb ($\phi_{\rm eff} = 1.9$ eV) resulting in a divergence term of $\sqrt{\mathrm{MTE}/m_o c^2} = 0.51$ mrad. The goal for the B*ERL*inPro injector is to deliver a projected emittance of $\varepsilon_{\rm proj} \leq 1$ mm mrad and slice emittance of $\varepsilon_{\rm slice} \leq 0.6$ mm mrad. To allow for some degradation due to non-linear processes, the target for the thermal emittance is $\varepsilon_{\rm th} = 0.3$ mm mrad. This can be achieved with initial spot size of $\sigma_{\rm in} = 0.6$ mm, resulting in a space-charge limited launch field of $E_l|_{\rm scl} = 5$ MV/m. The gun should be operated at least a factor of two away from this limit to allow for acceleration of the complete bunch including the tail particles. Therefore the launch field the cavity has to

* The work is supported by Bundesministerium für Bildung und Forschung and Land Berlin.
† kamps@helmholtz-berlin.de

ISBN 978-3-95450-122-9

supply is $E_l \geq 10$ MV/m. The ratio of launch-to-peak field in the cavity also wants to be high to reduce the propability of dark current production due to field emission.

The final state of the emittance is the result of a dynamic evolution under the influence of various forces. These forces can be electro-magnetic fields of the solenoid and SRF cavity as well as space-fields due to Coulomb repulsion. The normalized emittance at the injector exit can be summarized as the root-square sum of the individual contributions.

$$\varepsilon_n = \sqrt{\varepsilon_{\mathrm{th}}^2 + \varepsilon_{\mathrm{sol}}^2 + \varepsilon_{\mathrm{sc}}^2 + \varepsilon_{\mathrm{rf},\parallel}^2 + \varepsilon_{\mathrm{rf},\perp}^2} \qquad (2)$$

For now, we neglect the interaction between the beam and the cavity itself and due to higher-order modes and thus all transverse rf contributions to $\varepsilon_{\mathrm{rf},\perp}$. The contribution from space-charges forces $\varepsilon_{\mathrm{sc}}$ scales linearly with the peak beam current and therefore inversely with the laser pulse length. The contribution from longitudinal rf fields $\varepsilon_{\mathrm{rf},\parallel}$, mainly the slope and curvature of the accelerating field, scale quadrically or cubically with the pulse length. Consequently there exists an optimum pulse length at which the emittance is balanced between the two effects. Generally, the optimal pulse length is on the order of 10 degress of rf phase [5]. Projected emittance growth is caused by effects leading to mismatch of the motion in phase space of individual slices of the bunch. This type of emittance groth can be fixed by emittance compensation [6]. In this process, a solenoidal lens is used to remove linear correlations between the transverse and longitudinal phase space. Slice emittance growth, caused by non-linear space-charge forces or aberrations in optical elements, cannot be fixed by emittance compensation and needs to be suppressed by design of the gun cavity and the solenoid. The key is to start with a constant charge distriution, thus motivating complex longitudinal shaping of the drive laser pulse. Emittance growth caused by longitudinal rf effects can be mitigated by a proper field balance and by reduction of the initial pulse length.

Aberrations in the solenoid are a cause for slice emittance growth $\varepsilon_{\mathrm{sol}}$. Emittance growth by spherical aberrations scale quadratically with the transverse spot size. Hence we want to keep the transverse spot size in the solenoid small. This can be achieved by moving the solenoid closer to the SRF gun cavity and by focusing the beam during emission with radial electric field components of the accelerating field. This rf focusing is achieved by retracting the cathode out of the cavity backplane by a distance Δz_{cath}, usually by 1 to 3 mm [7]. By doing so, the electric field has a radial focussing component, which increases linearly in longitudinal direction and supplies the low energy electrons with initial focusing. Obviously this reduces the launch field and the launch-to-peak field ratio.

Conclusion for the cavity design

For the cavity design we can conclude from these considerations that the launch field during electron emission should be $E_l \geq 10$ MV/m with a high launch-to-peak field ratio and that the cathode should be retractable to achieve initial rf focusing.

SRF CAVITY OPTIONS

In this section we will evaluate several cavity options build and under considerations against the criteria setup in the previous section.

The purpose of the SRF gun cavity is to accelerate the electrons from almost zero energy to an energy as high as possible. An SRF gun cavity consits of a half cell with embedded cathode plus a varying number of full cells. Due to technical choices made in the design process, the average power delivered to the beam cannot exceed 230 kW [1]. At 100 mA beam current this means that the exit energy from the gun must be below 2.3 MeV. The launch field depends on the maximum field on axis E_{max}, the cathode-to-maximum field ratio G_{FF} and the launch phase according to $E_l = E_{max} \cdot G_{\mathrm{FF}} \cdot \sin\phi_l$. The maximum-to-peak field ratio is for all cavity designs under consideration $E_{pk}/E_{max} = 1.5$. Complementary studies focused on the RF properties indicate that a SRF gun cavity with a length of $1.n \cdot \lambda_{rf}/2$ with $0.4 < n < 0.6$ offers good performance with regard to field flatness and peak field on the metal surface [13]. In Table 1 launch fields and phases derived from simulations of phase scans are summarized for different design candidates. Listed are entries for the cavity employed at Gun0 [8, 9, 10] with 1.6cells, for the CDR baseline design [11] and three candidates for Gun1 (with 0.4 and 1.4cells [13]). Two entries for different values of cathode surface retraction Δz_{cath} are given for the 1.4cell design. The short cavities with 0.4 and 0.6 cells offer only low launch-to-peak field ratios togther with low absolute launch field levels. Therefore we will concentrate on a cavity design with 1.4 cells to study the effect of longitudinal laser pulse shaping.

Table 1: Cavity field parameters relevant for beam dynamics studies for 2 MeV target exit energy. See text for explanation of the parameters.

No.	Δz_{cath} mm	G_{FF}	E_{max} MV/m	ϕ_l degL	E_l MV/m
Gun0 1.6	0	0.99	21	27	9.4
CDR 0.6	-1.5	0.74	44	15	8.4
Gun1 0.4	-1.0	0.82	48	21	14.0
Gun1 1.4	-1.5	0.79	26	41	13.4
Gun1 1.4	-2.0	0.69	26	39	11.3

ADDING LONGITUDINAL LASER PULSE SHAPING

The beam quality from a photoemission electron gun is strongly dependent upon the transverse and longitudinal shape of the drive laser pulse. For lowest transverse emittance, the B*ERL*inPro baseline design requires a uniformly filled round transverse distribution and flat-top longitudinally. However since longitudinal laser pulse shaping is a technical challenge, it is important to study with simulations the effect of laser shaping on the transverse beam emittance. Fig. 2 shows the result of optimization runs leading to emittance compensation for Gaussian and Plateau shaped pulses at peak current of $I_{pk} = 5$ A. The

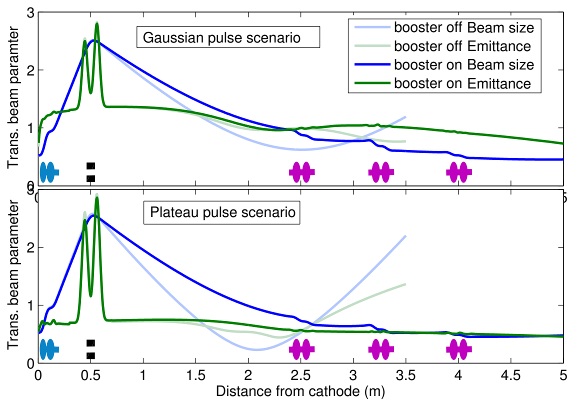

Figure 2: Transverse beam parameters for Gaussian and Plateau shaped drive laser profiles. Results are shown for booster on and off situations. The solenoid focal length has been slightly adjusted to optimize the matching of the beam into the booster.

Gaussian pulse has a rms length of $\sigma_t = 6$ ps, the Plateau shaped pulse has 1.8 ps rise/fall time and 18 ps width. The goal is to keep the rms pulse length constant from the cathode to the merger section of the ERL. The initial transverse spot size is round with 0.5 mm rms radius and the same for the two scenarios. The target beam parameters can be reached with both pulse shapes, the Plateau pulse setup outperforms the Gaussian shaped pulse by 20% with respect to projected emittance and linearity of the longitudinal and transverse phase space distribution.

Complete injector setup

A booster linac is added to gun and solenoid. The booster consits of three 2cell cavities of Cornell design [12]. The first cavity is located at the working point which results from the emittance compensation process. The goal is to effectivly freeze in the slice oscillation by increasing the beam energy to a level where the phase advance of the individual slices is not any more dominated by space-charge forces. The proposed setup may serve as guideline for the construction process of a realistic gun and booster setup. The gradient in the first cavity is set according to the invariant envelope criterion [14] to $E_{\mathrm{bc1}} = 7$ MV/m increasing the beam energy from 2.25 to 3 MeV. The two subsequent cavities each are set to $E_{\mathrm{bc2,3}} = 17.5$ MV/m to add 2 MeV resulting in an injector exit energy of 7 MeV. Here the emittance oscillations are effectively damped as can be seen in Fig. 2 for Gaussian

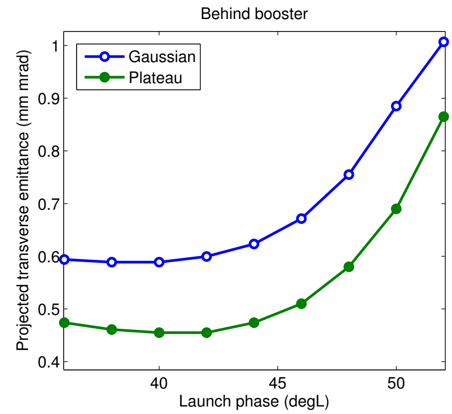

Figure 3: Transverse beam parameters for complete injector setup with initial Gaussian and Flat-top drive laser profile.

and Plateau drive laser profiles. The minium emittance at the end of the injector is a function of the launch phase as can be seen in Fig. 3

SUMMARY AND OUTLOOK

The goals for the B*ERL*inPro baseline beam parameter set can be reached with at 1.4cell cavity with retractable cathode design. With Plateau shaped bunches the performance with respect to the transverse beam emittance improves by more than 20% compared to Gaussian bunches. The next step is to move towards fully 3D simulation including all transverse rf effects from coupler kicks, higher-order modes and wakefields.

ACKNOWLEDGEMENTS

The authors acknoledge many fruitful discussions with M. Abo-Bakr, D. Dowell (SLAC/LBL), J. Sekutowicz (DESY), J. Teichert and A. Arnold (both HZDR).

REFERENCES

[1] The BERLinPro Conceptual Design Report (CDR), Eds.: A. Jankowiak, J. Knobloch, B. Kuske and N. Paulick

[2] K. Flöttmann, ASTRA V3 (2011)

[3] D. Dowell, SLAC-PUB-13535

[4] P. Kneisel, et al., Proc. of PAC 2010

[5] K. J. Kim, NIM A 275 (1989) 201

[6] B. E. Carlsten, NIM A 285 (1989) 313

[7] D. Janssen and V. Volkov, NIM A 452 (2000) 34

[8] A. Neumann, et al., Proc. of IPAC 2011

[9] T. Kamps, et al., Proc. of IPAC 2011

[10] J. Völker, et al., Proc. of IPAC 2012

[11] T. Kamps, Proc. of HBHAP 2009

[12] M. Liepe, et al., Proc. of SRF 2007

[13] A. Neumann, et al., Proc. of Linac 2012

[14] J. Rosenzweig and S. Serafini, Phys. Rev. E 55 6 (1997)

ISBN 978-3-95450-122-9